

# WASH-OUT CONDITIONS OF PLANTS GROWING ON ISLANDS BY FLOODS

Junji YAGISAWA<sup>1)</sup> and Norio TANAKA<sup>1)</sup>

<sup>1)</sup> Environmental and Hydraulic Lab., Department of Civil and Environmental Engineering, Saitama University

## ABSTRACT

To elucidate the wash-out conditions of plants in different locations on islands, the plant wash-out after two flood events was investigated and a two-dimensional depth-averaged unsteady flow model was applied to the Arakawa River, Japan. The simulation approximated the flood-water depth well. Then, the important parameters related to tree wash-out: (1) drag moment acting on trees, (2) bed shear stresses, and (3) dimensionless shear stresses of  $d_{50}(\tau_{*50})$  and  $d_{84}(\tau_{*84})$  were calculated using the simulated data and the bed material size determined in the field. Threshold drag moments and bed shear stresses for washing out representative vegetation, *Salix subfragilis*, *Robinia pseudoacacia*, *Eragrostis curvula*, and *Phragmites japonica*, on the islands were evaluated.

$\tau_{*84}$  was found to predict wash-out more accurately than the other parameters. Threshold values of  $\tau_{*84}$  when the trees near the riverside of the island were washed out were about 0.6–0.7 times of those on the flat area. Moreover, threshold values of  $\tau_{*84}$  for washing out grasses growing at the fringe area of the vegetation stand were 0.6–0.7 times those for grasses at the centre area. These results indicate that the threshold values for washing out plants depend on the location of vegetation in a river.

**KEYWORDS:** moment by drag force, shear stress, threshold of gravel movement, plant removal due to floods

## 1. INTRODUCTION

Vegetation in rivers creates valuable natural environments that maintain biodiversity. However, vegetation affects channel morphologies by increasing local roughness (Kouwen and Fathi-Morgan, 2000), obstructing flow (Wallerstein and Thorne, 2004), and providing sedimentation sites (Wyzga, 2001). On the other hand, by utilizing these effects, plants have also been used to prevent bank erosion in lakes (Sayah et al., 2004), rivers (Micheli and Kirchner, 2002), and places that are affected by ship waves (Bonham, 1983).

Forestation inside a river (Johnson, 1994) sometimes becomes a problem, not only because it reduces river flow capacity downstream, but because debris, i.e., broken tree trunks and branches, increase the drag force on bridge piers in rivers. When floating debris is attached to and accumulates around a pier, it causes a large scour hole around it and sometimes breaks the pier (Melville and Dongol, 1992). In addition, excessive forestation by a single tree species or an invasive exotic tree species sometimes affects the biodiversity of a river ecosystem (Stokes, 2008). For rejuvenation of a gravel bed river, information on how floods affect the formation of a plant community in a river is necessary. In particular, the characteristics of sand deposited by the flood event

(i.e., particle size, nutrient content) (Oswalt and King, 2005), flood disturbance frequency (Gilvear and Willby, 2006) and intensity (Vervuren et al., 2003), and bed degradation due to flooding (Kamrath et al., 2006) are reported to be important factors that affect the plant community.

Considering the above situation, it is necessary to elucidate the wash-out conditions of river vegetation due to floods. Conditions of plants uprooted by strong wind or flooding have been evaluated mainly in terms of drag moment acting on the plants (TRCRD, 1994; Gardiner et al., 2000) or bed shear stress (dimensionless shear stress) (Temple, 1980; Egger et al., 2007). However, the wash-out mechanisms of drag moment and shear stress are different. Moment acting on trees can wash out them by turning the root-anchoring zone of trees, whereas bed shear stress can wash out trees by reducing the tensile resistance between tree roots and bed substrate. However, the appropriate parameters to evaluate the wash-out condition of plants in rivers have not been quantitatively elucidated in previous research.

The wash-out condition of plants can be affected by the substrate characteristics of the vegetated area. For examples, Tanaka and Yagisawa (2008) conducted a field survey in the Tamagawa River in Japan after the flood of September 2007, and

reported that trees growing on the riverside of a gravel bar can be washed out easily in comparison with those growing on the flat area. On the other hand, trees growing close to potential failure plane locations are understood to reinforce the bank (Abernethy and Rutherford, 2000b). Plants growing near the bank side are reported to prevent bank erosion, but in some cases, plants growing near the bank are demonstrated to weaken bank stability by causing turbulence near the bank (McBride et al., 2007) and by the weight of trees growing on the river bank (Abernethy and Rutherford, 2000a). As shown in the above studies, the wash-out conditions of plants growing on the bank or riverside of an island are still not clear because the plants are located in unstable areas that are subject to erosion. It is necessary to distinguish the wash-out conditions of plants according to the location of the vegetation, i.e., the riverside or flat area of an island, because elucidation of the long-term conditions of vegetation is important.

Therefore, the objectives of this study were to clarify (1) the parameters applicable to evaluating the wash-out condition of plants growing in river, and (2) the difference in the wash-out conditions of plants in different locations on islands, i.e., riverside or flat area of an island and periphery or center of the vegetated area. To fulfill these objectives, the wash-out conditions of plants on two islands in the Arakawa River were investigated in detail after two flood events of October 2006 and September 2007.

## 2. MATERIAL AND METHODS

### 2.1 River flow analysis

River flow was analyzed by a continuity equation (Equation (1)) and two-dimensional depth-averaged Reynolds equations (Equations (2) and (3)). Porosity inside the vegetated area was considered in the continuity equation. The drag force due to vegetation was also included in the momentum equation (Takemura and Tanaka, 2005). These equations are

$$\theta \frac{\partial}{\partial t} \left( \frac{h}{J} \right) + \frac{\partial}{\partial \xi} \left( \frac{Uh}{J} \right) + \frac{\partial}{\partial \eta} \left( \frac{Vh}{J} \right) = 0 \quad (1)$$

$$\frac{\partial}{\partial t} \left( \frac{Q_x}{J} \right) + \frac{\partial}{\partial \xi} \left( \frac{UQ_x}{J} \right) + \frac{\partial}{\partial \eta} \left( \frac{VQ_x}{J} \right) = -gh \left( \frac{\xi_x}{J} \frac{\partial Z_x}{\partial \xi} + \frac{\eta_x}{J} \frac{\partial Z_x}{\partial \eta} \right) - \frac{\tau_x}{\rho J} - \frac{f_x}{\rho J} + \quad (2)$$

$$\frac{\xi_x}{J} \frac{\partial}{\partial \xi} (-u^2 h) + \frac{\xi_y}{J} \frac{\partial}{\partial \xi} (-u^2 v h) + \frac{\eta_x}{J} \frac{\partial}{\partial \eta} (-u^2 h) + \frac{\eta_y}{J} \frac{\partial}{\partial \eta} (-u^2 v h) \quad (3)$$

$$\frac{\partial}{\partial t} \left( \frac{Q_y}{J} \right) + \frac{\partial}{\partial \xi} \left( \frac{UQ_y}{J} \right) + \frac{\partial}{\partial \eta} \left( \frac{VQ_y}{J} \right) = -gh \left( \frac{\xi_y}{J} \frac{\partial Z_x}{\partial \xi} + \frac{\eta_y}{J} \frac{\partial Z_x}{\partial \eta} \right) - \frac{\tau_y}{\rho J} - \frac{f_y}{\rho J} + \quad (4)$$

$$\frac{\xi_x}{J} \frac{\partial}{\partial \xi} (-u^2 v h) + \frac{\xi_y}{J} \frac{\partial}{\partial \xi} (-v^2 h) + \frac{\eta_x}{J} \frac{\partial}{\partial \eta} (-u^2 v h) + \frac{\eta_y}{J} \frac{\partial}{\partial \eta} (-v^2 h)$$

where  $\theta$  is the porosity;  $t$  is the time;  $J$  is the Jacobian matrix;  $u$  and  $v$  are the depth-averaged velocities in  $x$  and  $y$  directions, respectively;  $U$  and  $V$  are the contra-variant velocity components of  $u$  and  $v$ , respectively;  $Q_x$  and  $Q_y$  are the contra-variant discharge fluxes in  $x$  and  $y$  directions, respectively;  $q_x$  and  $q_y$  are the discharge fluxes in  $x$  and  $y$

directions, respectively;  $\xi_x$ ,  $\xi_y$ ,  $\eta_x$ , and  $\eta_y$  are the matrices for coordinate conversion;  $\tau_x$  and  $\tau_y$  are the bed shear stresses in  $x$  and  $y$  directions, respectively;  $f_x$  and  $f_y$  are the drag forces per unit area in  $x$  and  $y$  directions, respectively;  $-\overline{u^2}$ ,  $-\overline{u^2 v}$ , and  $-\overline{v^2}$  are depth-averaged Reynolds stresses;  $g$  is the gravitational acceleration,  $h$  is the water depth,  $\rho$  is the fluid density; and  $Z_s$  is the water level.

To analyze the moment acting on a tree,  $M$ , we considered the drag force,  $F$ , including the tree stand structure (Tanaka et al., 2006) as shown in Equations (4) to (8), and bed shear stress,  $\tau$ , was evaluated by Equation (9).

$$f_x = \frac{1}{2} m \rho C_{d-ref} d_{BH} u \sqrt{u^2 + v^2} \int_0^h \frac{d(z)}{d_{BH}} \frac{C_d(z)}{C_{d-ref}} dz \quad (4)$$

$$f_y = \frac{1}{2} m \rho C_{d-ref} d_{BH} v \sqrt{u^2 + v^2} \int_0^h \frac{d(z)}{d_{BH}} \frac{C_d(z)}{C_{d-ref}} dz \quad (5)$$

$$F = \sqrt{f_x^2 + f_y^2} \quad (6)$$

$$\alpha(z) = \frac{d(z)}{d_{BH}}, \quad \beta(z) = \frac{C_d(z)}{C_{d-ref}} \quad (7)$$

$$M = \frac{1}{2} \rho C_{d-ref} d_{BH} (u^2 + v^2) \int_0^h z \alpha(z) \beta(z) dz \quad (8)$$

$$\tau = \sqrt{\tau_x^2 + \tau_y^2} = \sqrt{\left( \frac{\rho g n_b^2 u \sqrt{u^2 + v^2}}{h^{1/3}} \right)^2 + \left( \frac{\rho g n_b^2 v \sqrt{u^2 + v^2}}{h^{1/3}} \right)^2} \quad (9)$$

$$= \frac{\rho g n_b^2 (u^2 + v^2)}{h^{1/3}}$$

where  $z$  (m) is the vertical axis from the ground where trees are vegetated,  $m$  (number of trees/m<sup>2</sup>) is the tree density per unit area,  $C_{d-ref}$  is the reference drag coefficient (=1 considering a circular cylinder in this study),  $C_d(z)$ ,  $d(z)$  is the drag coefficient, cumulative width of tree trunks, and branches (m) at height  $z$ , respectively,  $d_{BH}$  is the tree trunk diameter at breast height (m),  $n_b$  (m<sup>-1/3</sup>s) is the Manning roughness coefficient without vegetation (assumed to be 0.035 in this study),  $\alpha(z)$  is an additional coefficient expressing the vertical tree structure, and  $\beta(z)$  is an additional coefficient representing the effect of leaves and the inclination of branches (for details, see Tanaka et al. (2006)).

The vertical distribution of  $\alpha(z)$  was estimated by image analysis. Image analysis was conducted for 12 *Salix subfragilis* stands and 14 *Robinia pseudoacacia* stands. The ages of these trees ranged between 1 and 10 years. For the value of  $\beta(z)$ , previous experiments indicated that the additional drag by leaves themselves can be assumed to be a constant value (1.25 (Fukuoka and Fujita, 1990) and 1.40 (Armanini et al., 2005)). Because the sensitivity of this parameter in calculating the breaking condition is not large, we used 1.25 for  $\beta(z)$ , assuming that the effects of the inclination of branches were larger than those in the condition of Armanini et al. (2005).

Table 1 Drag characteristics of each perennial grass was used in flow analysis

Species	Plant density $m$ (number of plants / m <sup>2</sup> )	Diameter of stem $D_c$ (m)	Plant height $h_v$ (m)	Drag coefficient $C_d$		
				$h_v / h^* < 0.8$ (submerged condition)	$0.8 < h_v / h^* < 1.0$ (submerged condition)	$h_v / h^* > 1.0$ (emergent condition)
<i>Eragrostis curvula</i>	1 <sup>†</sup>	0.3 <sup>††</sup>	1.2	0.3	0.3 - 1.0	1.0
<i>Phragmites japonica</i>	100	0.005	1.5	0.8	0.8 - 1.2	1.2
<i>Miscanthus sacchariflorus</i>	100	0.005	2.0	0.8	0.8 - 1.2	1.2

\*  $h$  is the water depth

<sup>†</sup>  $m$  of *E. curvula* is defined as number of clumps per m<sup>2</sup> in this study

<sup>††</sup>  $D_c$  of *E. curvula* is defined as outer diameter of a clump in this study

The Manning roughness coefficient with grass-type vegetation,  $n_w$ , was proposed by Petryk and Bosmajin (1975) as shown in Equation (10). The effect of additional roughness due to the grass-type vegetation was reflected in the numerical simulation as  $n_b = n_w$  in Equation (9).

$$n_w = \sqrt{n_b^2 + \frac{C_d}{2g} a_v X} \quad (10)$$

where  $a_v$  is the projected area of vegetation in a unit volume (m<sup>2</sup>/m<sup>3</sup>).  $X$  is changed by the ratio of shoot height of grass type vegetation ( $h_v$ ) and water depth ( $h$ ) (hereafter,  $h_v/h$  is called relative height). When the relative height was greater than 1 (emergent condition),  $X = h \times h_v^{1/3}$  was used, while  $X = h^{4/3}$  was used when it was smaller than 1 (submerged condition).

Tanaka et al. (2008, 2009) investigated the drag characteristics of clump-type roughness with different densities in flume experiments and indicated that the  $C_d$  value depended on the relative height. With reference to the experimental results of Takemura & Tanaka (2007) and Tanaka et al. (2008), the  $C_d$  value of grass-type vegetation was given to the numerical simulation as shown in Table 1. The plant density,  $m$ , plant diameter,  $d$ , and shoot height,  $h_v$ , of each grass type plant are also shown in Table 1.

## 2.2 Study area

A field investigation was conducted on two islands (Arakawa-ohashi (AR); 36°8'N, 139°22'E, Kumagaya-ohashi (KU); 36° 8'N, 139°20'E) located between 76 km and 82 km from the mouth of the Arakawa River, Japan (Figure 1). The bed forms in this river section are classified in the category changing from alternate bar to double row bar. The locations and shapes of these two islands have not much changed since 2000. The vegetation began to grow conspicuously on the investigated islands from 2000. It is rather difficult to identify the reasons for forest development in this river because many artificial alterations have been made to this river, e.g., bed degradation due to pick up the bed material from the riverside, a decrease in peak discharge during floods due to dam construction in upstream region of this river, and stabilization of the river channel due to the construction of many levees and weirs. However, the reason for the recent forestation of the investigated islands may be because no big flood

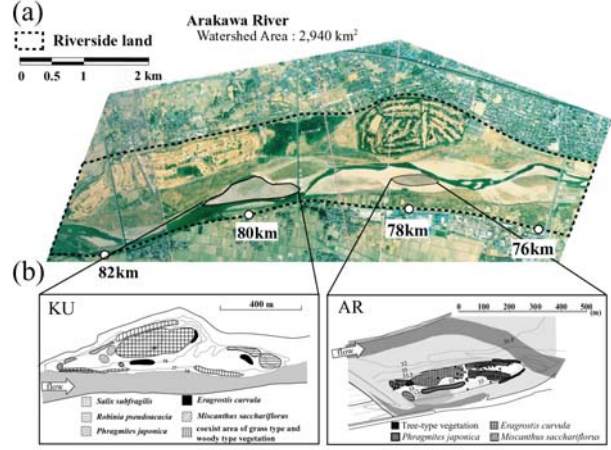


Figure 1 Location and vegetation map of two islands (AR and KU) in the Arakawa River after the 2007 flood; the numbers (76 km, 78 km, 80 km, 82 km) shown in Figure 1(b) indicate the distance from the river mouth.

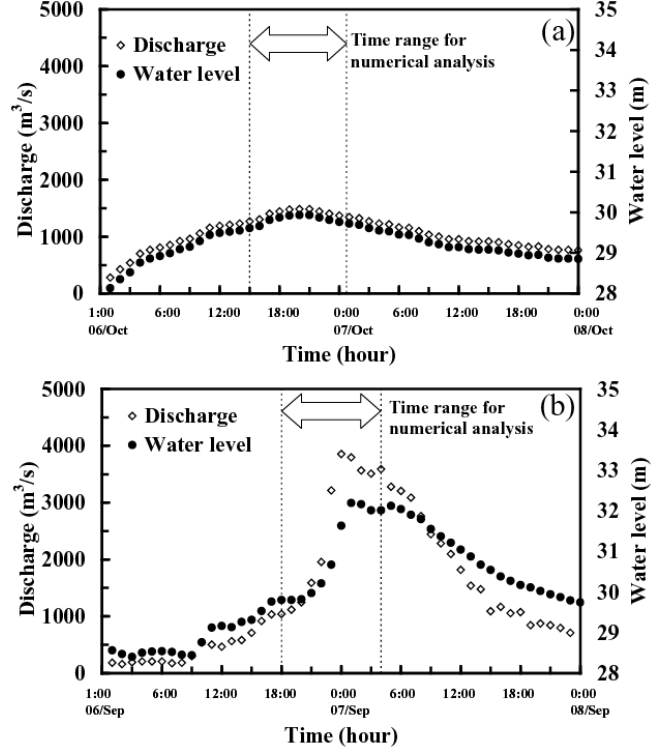


Figure 2 Observed discharge at the Uematsu-bashi gauge station (86 km from river mouth) and water level at the Kumagaya gauge station (76 km from river mouth) used for numerical simulation: (a) October 2006 flood, (b) September 2007 flood

had occurred since 2000. After 2005, when the field investigation of these islands was started, two floods occurred, one in September 2006 and one in October 2007. The recurrence intervals of the October 2006 flood and September 2007 flood were 3 years and 25 years, respectively. In the October 2006 flood, water level reached the top of each island. On the other hand, in the September 2007 flood, the water increased up to the top of each low channel (0.9 m above the island top). In the two floods with the characteristics mentioned above, the wash-out state of the dominant plants (*S. subfragilis*, *R. pseudoacacia*, *Phragmites japonica*, and *Eragrostis curvula*) on each island was investigated before and after these two flood events.

### 2.3 Size of bed material at two islands

Particle size distributions of river bed materials at AR and KU sites were determined at twenty and thirty locations, respectively.  $d_{50}$  and  $d_{84}$  were estimated by two methods in this study. One was to sample bed materials from the river bed surface to 5 cm depth and screen them by using five sieves with 31.7 mm, 19.1 mm, 9.52 mm, 5.66 mm, and 4.00 mm mesh to obtain the particle size distribution. The second was to take a photo of the river bed and conduct image analysis to determine the particle size distribution when the particle size is large and the screening test cannot be used. The range of  $d_{50}$  and  $d_{84}$  at the two islands were 1.8 cm to 11.1 cm and 3.2 cm to 14.0 cm, respectively.

### 2.4 Simulation of river flow

The observed flood discharge and water levels including the peaks at the October 2006 and September 2007 floods are given as the boundary conditions shown in Figure 2. The observed water level data at the Kumagaya gauge station located 76 km from the river mouth were taken as the downstream boundary. The observed discharge data at Uematsu-bashi gauge station located at 86 km from the river mouth could be taken as the upstream boundary, but the location of the upstream boundary was set at 82 km from the river mouth in this study. We judged that the numerical simulation expressed the flood situation well even if we moved the upstream boundary location for the calculation because there is a ground sill with a large potential head difference at 84 km from the river mouth that makes the numerical simulation unstable, and there is no tributary stream between the Uematsu-bashi gauge station (86 km) and the location of the upstream boundary in this study (82 km). The grid size used in numerical calculation was about 50 m long and 8 m wide, and the river bed elevation observed before September 2007 flood was averaged and set in each grid.

Tree-type plants (*S. subfragilis* and *R. pseudoacacia*) and grass-type plants (*E. curvula* and *P. japonica*) were considered in numerical

simulations by means of drag force (Equations (4)-(7)) and roughness (Equation (10)), respectively, although there were 15 species and 5840 trees on the island at KU. *S. subfragilis* and *R. pseudoacacia* comprised about 80% of all trees on this island, and the sensitivity of the tree shape differences was not large in the remaining 20%. The density of tree stands,  $m$ , tree height,  $h_v$ , and trunk diameter at breast height,  $d_{BH}$ , were investigated before the September 2007 flood and used for the simulation. The tree height and trunk diameter at breast height were averaged in each calculation grid and set.

### 2.5 Critical shear stress estimation for $d_{50}$ and $d_{84}$

To evaluate the shear stress acting on the grain,  $\tau_{*i}$ , the non-dimensionalized Shields parameter, which is usually used for considering ‘the gravity force (slope direction)’ over ‘the weight of the grain in water’, was calculated as below:

$$\tau_{*i} = \frac{\rho g H I_b}{(\rho_s - \rho) g d_i} = \frac{H I_b}{\left(\frac{\rho_s}{\rho} - 1\right) d_i} \quad (11)$$

where  $\rho_s$  and  $\rho$  are the density of the particles and water, respectively;  $g$  is the gravitational acceleration;  $d_i$  is the grain diameter at which  $i\%$  volume passes through the sieve, and  $I_b$  is the bed slope.

The critical shear stress of  $d_{50}$  for the initiation of motion,  $\tau_{*c50}$  can be approximated from the Shields diagram (i.e., Graf (1984)) as:

$$\frac{\tau_{*c50}}{(\rho_s - \rho) g d_{50}} = 0.06 \quad (12)$$

To calculate the effects of the grain size distribution, the critical shear stress of each grain size  $i$ ,  $\tau_{*ci}$ , as proposed by Egiazaroff (1965), was:

$$\frac{\tau_{*ci}}{(\rho_s - \rho) g d_i} = \frac{0.1}{[\log_{10} 19(d_i/d_m)]^2} \quad (13)$$

where  $d_m$  is the medium grain size. The parameters  $\tau_{*50}$  and  $\tau_{*84}$  are derived by substituting  $d_i = d_{50}$  or  $d_{84}$  in Equation (11), respectively, and  $\tau_{*c84}$  is derived by substituting  $d_i = d_{84}$  in Equation (13).

$d_{84}$  was selected for classifying the tree-breaking patterns including the bed degradation mechanism because: (1) the maximum grain diameter,  $d_{max}$ , and  $d_{84}$  are the dominant parameters used for expressing bedload transport (Blizard and Wohl (1998)), (2)  $d_{max}$  is difficult to determine from the sample (sample error is large), (3)  $d_{84}$  is related to the geometric standard deviation,  $\sigma_g = d_{84}/d_{50}$ , when the grain size distribution of bed material is expressed on a logarithmic scale (Otto, 1939), (4)  $d_{84}$  is used in empirical equations for estimating river morphology (i.e., depth of low channels and river bed gradient) (Hey and Thorne, 1986), and (5)

the local scour depth around bridge piers (similar to that around a tree trunk), including the armoring phenomena, is closely related to  $d_{84}$  and  $d_{50}$ .

### 3. RESULTS

#### 3.1 Comparison of simulated and observed water levels for the September 2007 flood

Contour maps of the simulated velocity and water depth at the peak discharge of the flood are shown in Figure 3. The inundations of flood areas “A (island at KU)” and “B (flood plain)” in Figure 3(c) were reproduced well in the simulation (Figure 3(b)). However, it was difficult to confirm that the result of the simulation was good enough to evaluate the situation of the flood as a two-dimensional expression. Therefore, validation of the numerical simulation was conducted by comparing the calculated and observed peak water levels (Figure 4). The maximum water level at the flood event was determined by the Ministry of Land, Infrastructure, Transport and Tourism of Japan (MLIT) by measuring the height at which debris was attached. The peak water level in the flood simulation was used as the maximum value at each calculation grid, and the calculations agreed well with the observed peak water level as a whole. The simulated peak water level in the areas with vegetation was around 15 cm higher at the upstream regions of AR and KU sites than that simulated under the assumption of lacking vegetation. As shown in Figure 3(c), almost all islands in the river channel were submerged, while the floodplain, with denser vegetation, was not submerged in the September 2007 flood. Therefore,

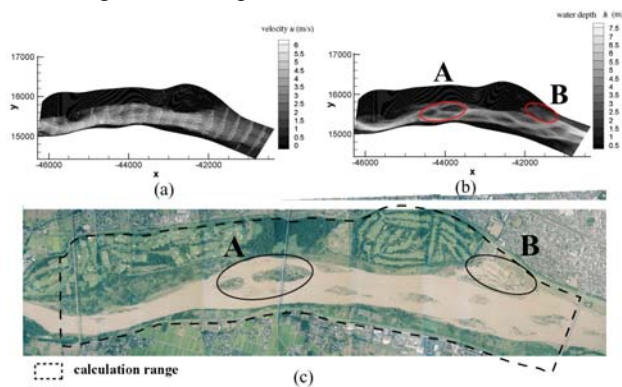


Figure 3 Flow situations of Arakawa River between 76 km to 82 km at the maximum discharge of the September 2007 flood: (a) contour and vector map of simulated velocity, (b) contour map of simulated water depth, (c) aerial photo (provided by Kanto Regional Development Bureau, Ministry of Land, Infrastructure, Transport and Tourism, Japan).  $x$  and  $y$  represent the axes in the orthogonal coordinate system. The two elements in Figure 3(c) representing the inundated areas are “A (island at KU)” and “B (flood plain)”.

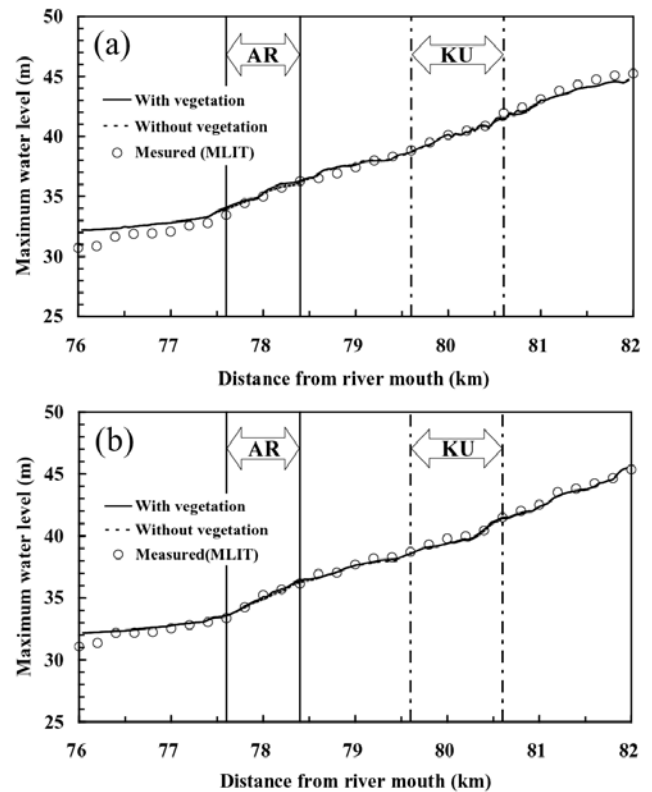


Figure 4 Comparison of simulated and observed maximum water levels along the Arakawa River during the September 2007 flood: (a) on the right bank, (b) on the left bank

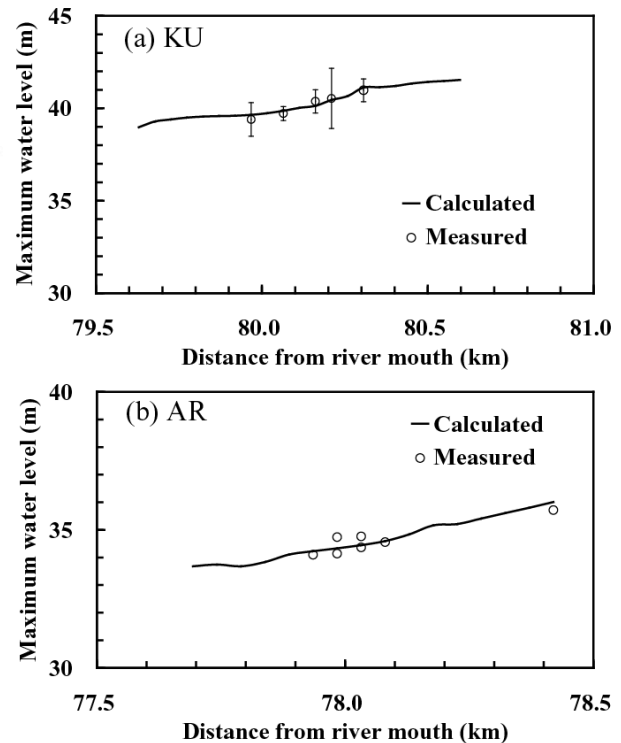


Figure 5 Comparison of simulated and observed maximum water levels along each island during the September 2007 flood: (a) KU, (b) AR. The vertical bars at each point represent the standard deviation.

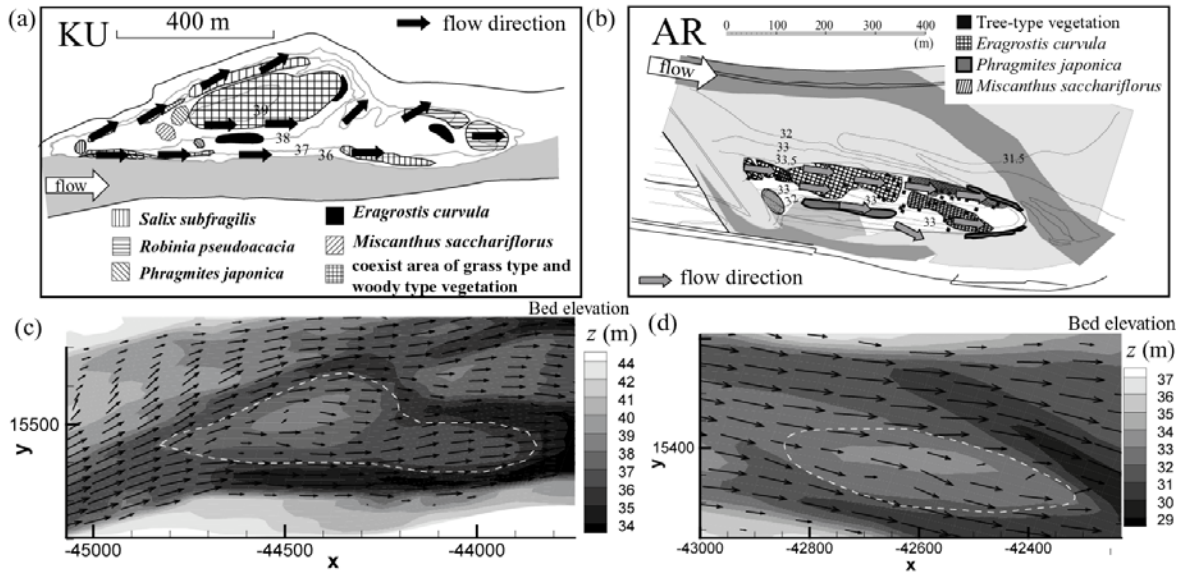


Figure 6 Comparison of simulated and observed velocity vectors of each island during the September 2007 flood: (a) observed velocity vectors at KU, (b) observed velocity vectors at AR, (c) calculated velocity vectors at KU, (d) calculated velocity vectors at AR. The broken lines in (c) and (d) represent the outer shape of each island.

there was little difference between the calculated peak water levels with and without vegetation.

The observed and simulated water levels on each island were compared at the peak discharge of the flood (Figure 5(a) and (b)). The observed water levels were determined by the heights of debris attached to trees. There was not much observed data because most of the trees were washed out or bent, but the calculations agreed well with the observed water level on each island. In Figure 6, the observed velocity vectors, which were determined from the direction of overturned plants, were compared with the calculated velocity vectors for each island. The calculations represent the observed velocity vectors of each island well. These results indicate that the numerical calculations used in this study express the two-dimensional flow situation at each island in the actual flood.

### 3.2 Evaluation of wash-out conditions of *S. subfragilis* and *R. pseudoacacia* by moment acting on tree trunks and shear stress at the bed

Figure 7 presents the relationship between the simulated moment acting on trees and simulated shear stress at the bed level during the 2006 and 2007 flood events. Closed and open symbols show whether the trees were washed out or not, respectively. In Figure 7, the range of critical moment for washing out trees,  $M_c$ , was defined between the maximum moment when trees were not washed out and the minimum moment when trees were washed out. This figure indicates that it is rather difficult to express the wash-out conditions for *S. subfragilis* and *R. pseudoacacia* as a single value of the moment acting on the trees.

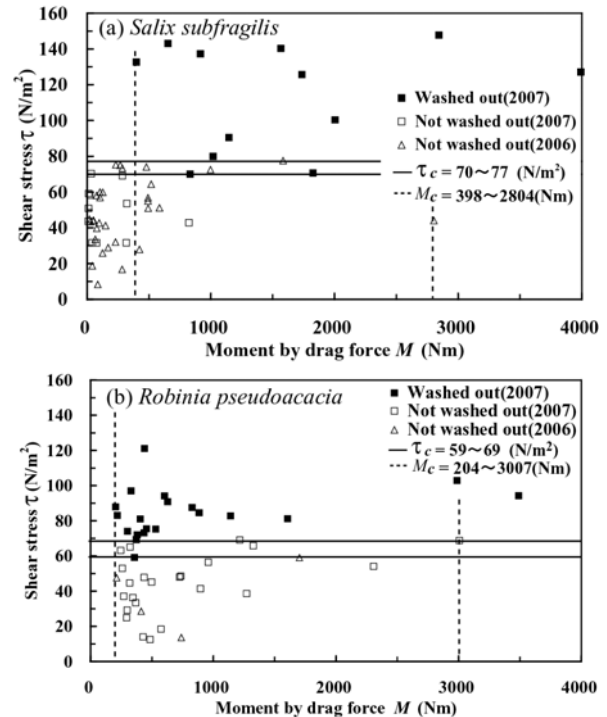


Figure 7 Relationship between moment acting on tree trunks and shear stress at the bed during the September 2007 and October 2006 floods: (a) *S. subfragilis*, (b) *R. pseudoacacia*.  $M_c$ : critical moment for washing out a tree,  $\tau_c$ : critical shear stress at the bed for washing out a tree, closed symbol: trees were washed out, open symbols: trees were not washed out.

The range of critical shear stress for washing out trees,  $\tau_c$ , is similarly defined as lying between the maximum shear stress at the vegetated area when trees were not washed out and the minimum shear stress when trees were washed out. The range of  $\tau_c$  is much narrower than the range of  $M_c$  and can be

estimated as 74–78 N/m<sup>2</sup> and 60–70 N/m<sup>2</sup> for *S. subfragilis* and *R. pseudoacacia*, respectively. Therefore, shear stress is a suitable indicator for classifying the wash-out condition of trees.

### 3.3 Critical shear stress for washing out *E. curvula* and *P. japonica* in different locations

The shear stress at the bed,  $\tau$ , and critical shear stress for washing out grass-type plants *E. curvula* or *P. japonica*,  $\tau_c$ , are shown in Figure 8, distinguishing the location in which the plants were growing, i.e., fringe region (FR) or centre region (CE). From this figure, the range of critical shear stress at the fringe ( $\tau_{c\_FR}$ ) and at the centre ( $\tau_{c\_CE}$ ) of *E. curvula* stand can be estimated as 58–60 N/m<sup>2</sup> and 76–120 N/m<sup>2</sup>, respectively. The ranges of  $\tau_{c\_FR}$  and  $\tau_{c\_CE}$  of *P. japonica* were also evaluated as 70–75 N/m<sup>2</sup> and 94–110 N/m<sup>2</sup>, respectively.

As the velocity and shear stress decrease inside a vegetated area (Kouwen and Unny, 1973), the apparent critical shear stress derived by the depth-averaged equation for washing out plants increases. The depth-averaged equation does not consider the difference between the flow velocity over the plants and through the vegetated zone. The difference increases as the flow passes through the vegetation (Righetti and Armanini, 2002). The actual shear stress at the centre of a vegetated area is assumed to be smaller than that at the fringe. Therefore, the critical shear stress for washing out plants at CE,  $\tau_{c\_CE}$ , is larger than that at FR,  $\tau_{c\_FR}$ .

### 3.4 Estimation of wash-out condition of plants on islands by non-dimensionalized shear stress

Figure 9(a)-(d) shows the relationship between  $\tau_{*50}/\tau_{*c50}$  and  $\tau_{*84}/\tau_{*c84}$  at the areas overgrown with *S. subfragilis* and *R. pseudoacacia* with emphasis on the difference between the flat region (FL) and the area near the riverside (RS) of the island. Figure 9(e)-(h) shows the relationship between  $\tau_{*50}/\tau_{*c50}$  and  $\tau_{*84}/\tau_{*c84}$  at the vegetated area of *E. curvula* and *P. japonica* with emphasis on the difference between the FR and CE of the vegetation. In Figure 9, the range of critical values of  $\tau_{*50}/\tau_{*c50}$  and  $\tau_{*84}/\tau_{*c84}$  for washing out the plants by flooding were defined as laying between the maximum values of  $\tau_{*50}/\tau_{*c50}$  and  $\tau_{*84}/\tau_{*c84}$  near the plant when plants were not washed out and the minimum values of  $\tau_{*50}/\tau_{*c50}$  and  $\tau_{*84}/\tau_{*c84}$  near the plant when plants were washed out. In each graph of Figure 9, the range of critical values of  $\tau_{*84}/\tau_{*c84}$  is narrower than that of  $\tau_{*50}/\tau_{*c50}$ . In poorly sorted gravels, as in this study site ( $d_{84}/d_{50}=1.6-2.8$ ), bed degradation or local scour around plants may be limited by the armoring phenomenon (Breusers et al., 1977). Therefore,  $\tau_{*84}/\tau_{*c84}$  is a suitable indicator for classifying the wash-out condition of plants on an island. Figure 9(a)-(d) shows that the ranges of  $\tau_{*84}/\tau_{*c84}$  on the flat area and the riverside of the island for *S. subfragilis* are 1.2–1.4 and 0.7–0.9,

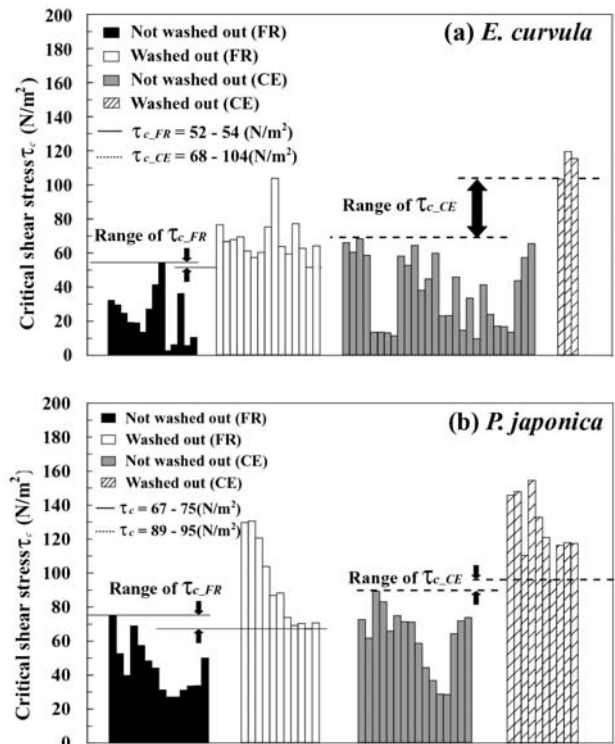


Figure 8 Difference of critical shear stress,  $\tau_c$ , for two grass species between different locations of the vegetation (CE: centre of the vegetated area, FR: fringe of the vegetated area): (a) *E. curvula*, (b) *P. japonica*.  $\tau_{c\_FR}$  and  $\tau_{c\_CE}$  represent the critical shear stress for washing out plants growing on the fringe (FR) and at the centre (CE) of the vegetation stand, respectively.

respectively. On the other hand, the ranges of  $\tau_{*84}/\tau_{*c84}$  on the flat area and riverside of the island for *R. pseudoacacia* are 0.9–1.2 and 0.6–0.8, respectively. These results indicate that the critical value of  $\tau_{*84}/\tau_{*c84}$  for washing out plants at the riverside is lower than that at flat area. The critical value of  $\tau_{*84}/\tau_{*c84}$  for washing out plants should be distinguished with the different location of the island. Tanaka and Yagisawa (2009) conducted field investigations in the Tamagawa River, Japan, after the September 2007 flood and reported that most of the trees washed out by the floods were trees growing near the riverside of the island.

Figure 9(e)-(h) shows that the ranges of  $\tau_{*84}/\tau_{*c84}$  at the fringe and centre areas of the *E. curvula* stand were 0.9–1.2 and 1.2–1.7, respectively. On the other hand, the ranges of  $\tau_{*84}/\tau_{*c84}$  at the fringe and centre areas of the *P. japonica* stand were 1.3–1.4 and 1.9–2.1, respectively. Thus, the critical value of  $\tau_{*84}/\tau_{*c84}$  for washing out the two species at CE was larger than that at FR. These results indicate that the critical values of  $\tau_{*84}/\tau_{*c84}$  at the fringe and centre regions of the vegetated areas should be distinguished when evaluating the wash-out condition of a

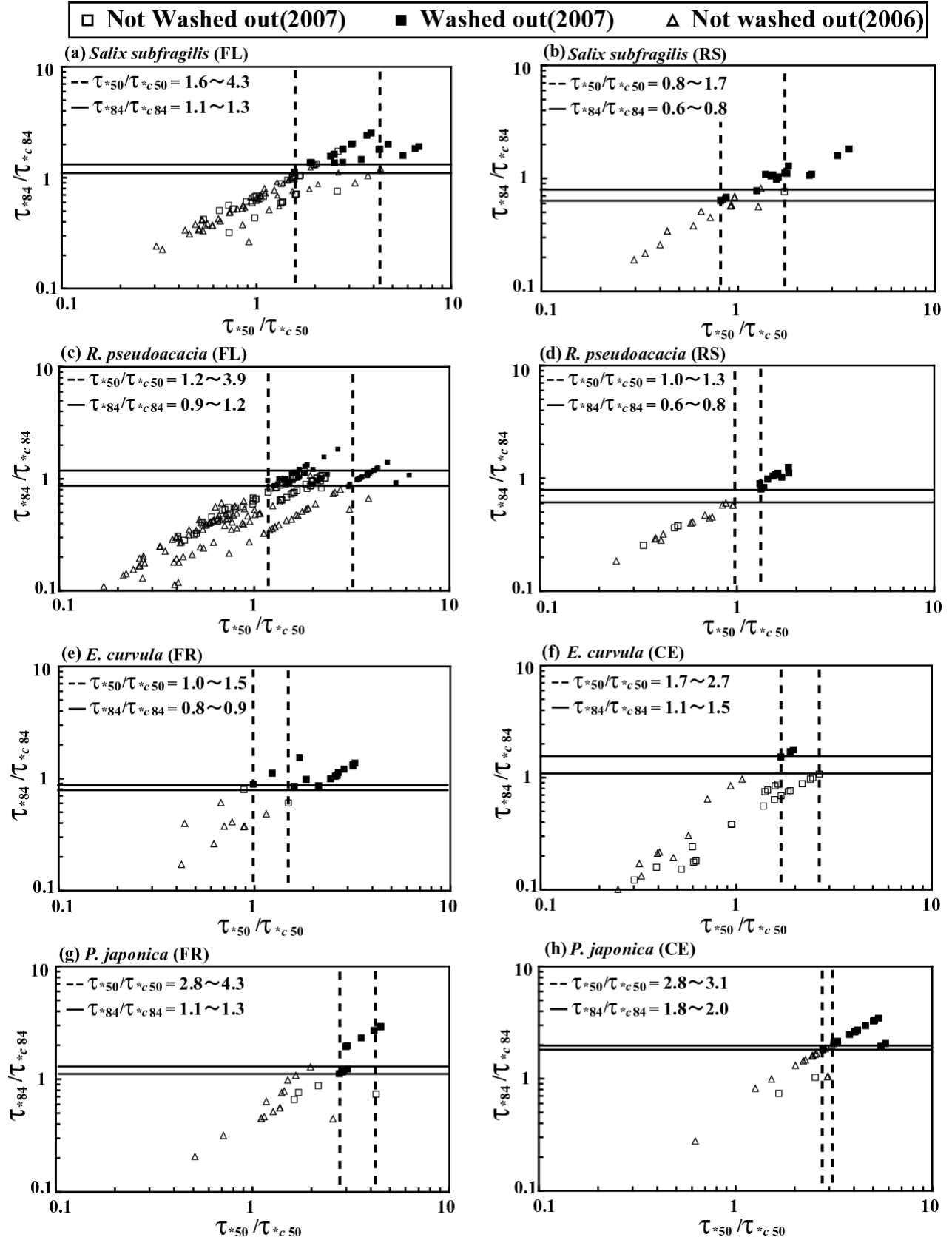


Figure 9 Difference between critical values of  $\tau_{*50}/\tau_{*c50}$  and  $\tau_{*84}/\tau_{*c84}$  for washing out plants growing at different locations: (a) *S. subfragilis* at FL, (b) *S. subfragilis* at RS, (c) *R. pseudoacacia* at FL, (d) *R. pseudoacacia* at RS, (e) *E. curvula* at FR, (f) *E. curvula* at CE, (g) *P. japonica* at FR, and (h) *P. japonica* at CE. FL and RS represent the vegetation located on a flat area and near the riverside on an island, respectively. CE and FR denote centre and fringe of the vegetated area, respectively.

clump-type grass *E. curvula* and a perennial plant *P. japonica*, respectively, due to floods.

## 4. DISCUSSION

### 4.1 Suitable indicator for classifying wash-out condition of plants on the island

A suitable index for evaluating the wash-out conditions of plants on an island is discussed below in terms of moment by drag force, shear stress at the bed, and non-dimensionalized shear stress.

As shown in Figure 7, when the wash-out condition of trees is evaluated by moment, the range of critical values of the parameter is wide because the difference in particle diameters around trees greatly affects the erosion (Tanaka and Yagisawa 2009). The critical moment for washing out trees on an island with large-diameter gravel was quite a bit larger than that on a sand or silty deposited layer (Tanaka and Yagisawa, 2009). In those conditions, the trees investigated in this study were washed out by severe bed degradation or local scour before the moment acting on a tree exceeded the critical value for washing out. Therefore, shear stress at the bed expressed better the wash-out condition of trees in comparison with the moment acting on trees. However, if the river bed materials around a tree are compacted or highly cohesive and have high critical shear strength for entrainment, the wash-out condition of trees is not decided by the shear stress alone. In that case, the moment acting on trees can be more important than the shear stress at the bed. Further studies are needed to elucidate the critical wash-out condition of trees growing on floodplains in the future.

Egger et al. (2007) evaluated the critical shear stress ( $\tau_c$ ) for washing out young willows. In their study, the  $\tau_c$  of young willows was 10 N/m<sup>2</sup>. However, in the present study, the  $\tau_c$  of *Salix* spp. was about 8 times larger (=78 N/m<sup>2</sup> (Figure 7(a))). This indicates that the value of  $\tau_c$  should depend on the bed materials occurring in different vegetation locations within a river, even if the  $\tau_c$  is derived for the same species. Blizard and Wohl (1998) noted that  $d_{max}$  or  $d_{84}$  is a dominant parameter for bed load transportation, and that particle diameter of bed materials can greatly influence the depth of bed degradation. When the wash-out of trees on islands is assumed to have occurred due to bed degradation around the trees, the Shields parameter ( $\tau^*$ ) can be more suitable parameter for evaluating the wash-out condition of trees than  $\tau_c$ , which is affected greatly by the particle diameter of bed materials.

In this study,  $\tau_{*84}/\tau_{*c84}$  expressed the wash-out condition more accurately than  $\tau_{*50}/\tau_{*c50}$  because the bed materials were relatively poorly sorted and the ratio  $d_{84}/d_{50}$  was large. Melville and Sutherland (1988) investigated the local scour depth around a bridge pier, similar to a tree trunk shape, and suggested that the depth is closely related to  $d_{84}$  and

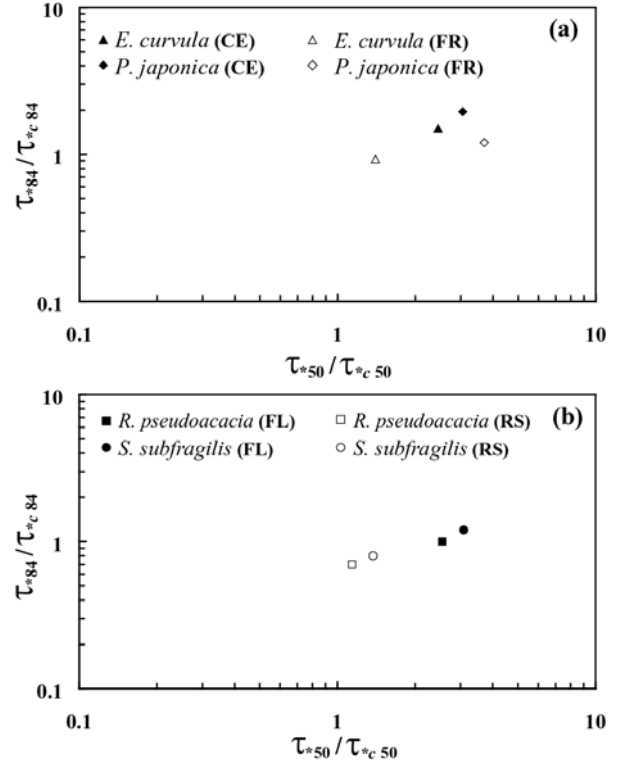


Figure 10 Relationship between the critical values of  $\tau_{*50}/\tau_{*c50}$  and  $\tau_{*84}/\tau_{*c84}$  for washing out plants: (a) comparison of *E. curvula* and *P. japonica* (closed plots: near centre region of the vegetated area, CE), open plots: fringe region, FR). (b) comparison of *R. pseudoacacia* and *S. subfragilis* (closed plots: flat area of the island, FL), open plots: the side of the island, RS).

$d_{50}$ . If  $d_{84}/d_{50}$  is almost equal to 1, the wash-out condition of plants may be evaluated accurately even if  $\tau_{*50}$  is used. However, for poorly sorted sediments, with the ratio  $d_{84}/d_{50}$  markedly greater than 1,  $\tau_{*84}/\tau_{*c84}$  can classify the wash-out condition of plants better than  $\tau_{*50}/\tau_{*c50}$  because the bed degradation is controlled by large-size particles, such as  $d_{84}$ .

### 4.2 Effect of critical value of $\tau_{*84}/\tau_{*c84}$ on wash-out of plants in different locations

The critical values of  $\tau_{*84}/\tau_{*c84}$  in Figure 9 are rearranged in Figure 10. Figure 10(a) shows the relationship between the averaged critical values of  $\tau_{*50}/\tau_{*c50}$  and  $\tau_{*84}/\tau_{*c84}$  for washing out *P. japonica* and *E. curvula*. Closed and open plots distinguish whether the plants are growing near the centre or fringe region of the vegetated area, respectively. Bars show the standard deviation of  $\tau_{*50}/\tau_{*c50}$ . For  $\tau_{*84}/\tau_{*c84}$ , only the average value is plotted for simplicity, because the standard deviation of this parameter is not much larger than the symbol size (Figure 9). In this figure, we found that the critical value of  $\tau_{*84}/\tau_{*c84}$  for washing out *P. japonica* is larger than that of *E. curvula* in two locations, the fringe and centre regions of the vegetated area. The

difference in the critical value of  $\tau_{*84}/\tau_{*c84}$  between the species is assumed to be caused by the difference between the root systems of *E. curvula* and *P. japonica*. The roots of *E. curvula* penetrate more deeply than those of other annual herbaceous plants. However, *P. japonica* has extensive belowground organs, rhizomes and roots, that bind the substrate. The soil binding effect of roots (Gradzinski et al. 2003) of *E. curvula* is supposed to be weak in comparison with that of *P. japonica*. Thus, the critical value of  $\tau_{*84}/\tau_{*c84}$  for the wash-out of *E. curvula* is less than that for *P. japonica*. Figure 10(b) shows the relationship between the average critical values of  $\tau_{*50}/\tau_{*c50}$  and  $\tau_{*84}/\tau_{*c84}$  for washing out *S. subfragilis* and *R. pseudoacacia*. The critical value of  $\tau_{*84}/\tau_{*c84}$  for the wash-out of *S. subfragilis* is larger than that of *R. pseudoacacia* in two locations, the flat area and the riverside of the island. The tree ages and trunk diameters at breast height of the *S. subfragilis* and *R. pseudoacacia* growing in this study site were  $3\pm 2$  years (sample size (ns) = 1935) and  $2.8\pm 7.2$  cm (ns = 1935) and  $4\pm 2$  years (ns = 2259) and  $3.8\pm 2.6$  cm (ns = 2259), respectively. Thus, *S. subfragilis* tended to be younger than *R. pseudoacacia*. Nevertheless the critical value of  $\tau_{*84}/\tau_{*c84}$  for the wash-out of *S. subfragilis* was higher than that for *R. pseudoacacia*. This is because the rhizosphere of *S. subfragilis* is deeper in comparison with *R. pseudoacacia*. The root penetration depths of *S. subfragilis* and *R. pseudoacacia* growing in this study site were  $78.5\pm 20.5$  cm (ns = 10) and  $51.0\pm 8.9$  cm (ns = 12), respectively. The critical value of  $\tau_{*84}/\tau_{*c84}$  for the wash-out of *S. subfragilis*, which has a greater root penetration depth, was larger than that for *R. pseudoacacia* with a shallow root penetration depth. Micheli and Kirchner (2002) investigated the effect of vegetation on bank strength, and indicated that a “wet meadow” with deep root penetration can increase the tensile strength of bank soils more in comparison with a “dry meadow” with shallow root penetration. Van de Wiel and Darby (2007) also indicated that the depth and distribution of rhizospheres greatly affect the stability of a river bank. Finally, Abernethy and Rutherford (2000a) indicated that the weight of riparian trees may contribute to the instability of a river bank. As shown in Figure 10(b), trees growing at the riverside of the island were washed out even if  $\tau_{*84}/\tau_{*c84}$  was less than 1 because the threshold of tree wash-out is not decided by bed degradation alone there.

## 5. CONCLUSIONS

The capabilities of threshold drag moments, shear stresses at the bed, and non-dimensionalized shear stresses of  $d_{50}$  and  $d_{84}$  to wash out representative vegetation growing on islands were evaluated using results of the numerical simulation of two floods and the wash-out condition at the site.

As a result, we determined that the non-dimensionalized shear stress of  $d_{84}$ ,  $\tau_{*84}$ , could evaluate the wash-out condition more accurately than the other parameters.

The critical values of  $\tau_{*84}/\tau_{*c84}$  for washing out representative trees growing on the flat and riverside areas of an island were elucidated. In addition, the critical values of  $\tau_{*84}/\tau_{*c84}$  for washing out representative grasses at the fringe and centre areas of the vegetation stand were also evaluated. The threshold value of  $\tau_{*84}/\tau_{*c84}$  for washing out trees growing near the riverside was only 0.6–0.7 times that of trees on the flat area. Moreover, the threshold value of  $\tau_{*84}/\tau_{*c84}$  for washing out grasses at the fringe area of the vegetation stand was 0.6–0.7 times that of grasses growing on the centre area.

This study suggests that the critical value of  $\tau_{*84}/\tau_{*c84}$  for washing out plants growing on an island may be changed greatly by the penetration depth or distribution of roots. More investigations are necessary to elucidate the relationship between the characteristics of plant root systems and the critical value of  $\tau_{*84}/\tau_{*c84}$  for washing out trees and grasses.

## 6. ACKNOWLEDGEMENTS

The Kanto Regional Development Bureau, Ministry of Land, Infrastructure, Transport and Tourism, Japan, is acknowledged for sharing the valuable data they observed.

## 7. REFERENCES

- Abernethy B, Rutherford ID. (2000a). “The effect of riparian tree roots on the mass-stability of riverbanks”, *Earth Surf. Process. Landforms*, **V. 25**, pp.921-937.
- Abernethy B, Rutherford ID. (2000b). “Does the weight of riparian trees destabilize riverbanks?”, *Regul. Rivers: Res. Mgmt.* **V.16**, pp.565-576.
- Armanini A, Righetti M, Grisenti P. (2005). “Direct measurement of vegetation resistance in prototype scale”, *J. Hydraulic Research* **V.43**, pp.481-487.
- Blizard CR, Wohl EE. (1998), “Relationships between hydraulic variables and bedload transport in a subalpine channel, Colorado Rocky Mountains, U.S.A.”, *Geomorphology* **V.22**, pp.359-371.
- Bonham AJ. (1983), “The management of wave-spending vegetation as bank protection against boat wash”, *Landscape and Urban Planning*, **V.10(1)**, pp.15-30.
- Breusers HNC, Nicollet G, Shen HW. (1977), “Local scour around cylindrical piers”, *J. Hydraulic Research* **V.15**, pp.211-252.
- egger E, Benjankar R. Davis L, Jorde K. (2007), “Simulated effects of dam operation and water diversion on riparian vegetation of the lower Boise river Idaho, USA.”, *32<sup>nd</sup> IAHR Congress* (CD-ROM).

- Egiazaroff JV. (1965), "Calculation of Nonuniform sediment concentrations", *Proc. Am. Soc. Civil Engineers*, **V.91(4)**, pp.225-247.
- Fukuoka S, Fujita K. (1990), "Hydraulic effects of luxuriant vegetations on flood flow (in Japanese with English abstract)", Report of PWRI, **V.180(3)**, p.64.
- Gardiner B, Peltola H, Kellomäki S. (2000), "Comparison of two models for predicting the critical wind speeds required to damage coniferous trees", *Ecological Modelling*, **V.129**, pp.1-23.
- Gilvear D, Willby N. (2006), "Channel dynamics and geomorphic variability as controls on gravel bar vegetation: river Tummel, Scotland", *River Res. Applic.*, **V.22**, pp.457-474.
- Gradziński R, Baryła J, Doktor M, Gmur D, Gradziński M, Kędzior A, Paszkowski M, Soja R, Zieliński T, Żurek S. (2003), "Vegetation-controlled modern anastomosing system of upper Narew River (NE Poland) and its sediments", *Sedimentary Geology*, **V.157**, pp.253-276.
- Graf WH. (1984), "Hydraulics of sediment transport. Water Resources Publications", LLC, p.97.
- Hey RD, Thorne R. (1986), "Stable channels with mobile gravel beds", *J. Hydraulic Engineering*, **V.112(8)**, pp.671-689.
- Johnson WC. (1994), "Woodland expansion in the Platte River, Nebraska: patterns and causes", *Ecological Monographs*, **V.64(1)**, pp.45-84.
- Kamrath P, Rubbert S, Köngeter J. (2006), "The effects of bottom settlement, vegetation and macro-roughness on the erosion stability of the relocated River Inde", *J. River Basin Management*, **V.4(1)**, pp.31-38.
- Kouwen N, Fathi-Morgan M. (2000), "Friction factors for coniferous trees along rivers", *J. Hydraulic Engineering*, **V.126(10)**, pp.732-740.
- Kouwen N, Unny TE. (1973), "Flexible roughness in open channels", *J. Hydraulics division*, **V.99**, pp.713-728.
- McBride M, Hession WC, Rizzo DM, Thompson DM. (2007), "The influence of riparian vegetation on near-bank turbulence: a flume experiment", *Earth Surf. Process. Landforms*, **V.32**, pp.2019-2037.
- Melville BW, Dongol DM. (1992), "Bridge pier scour with debris accumulation", *J. Hydraulic Engineering*, **V.118(9)**, pp.1306-1310.
- Melville BW, Sutherland AJ. (1988), "Design method for local scour at bridge piers", *J. Hydraulic Engineering*, **V.114(10)**, pp.1210-1226.
- Micheli ER, Kirchner JW. (2002), "Effects of Wet Meadow riparian vegetation on streambank erosion. 2. measurements of vegetated bank strength and consequences for failure mechanics", *Earth Surf. Process. Landforms*, **V.27**, pp.687-697.
- Oswalt SN, King SL. (2005), "Channelization and floodplain forests: Impacts of accelerated sedimentation and valley plug formation on floodplain forests of the Middle Fork Forked Deer River, Tennessee, USA.", *Forest Ecology and Management*, **V.215**, pp.69-83.
- Otto GH. (1939), "A modified logarithmic probability graph for the interpretation of mechanical analyses of sediments", *Journal of sedimentary petrology*, **V.9(2)**, pp.62-72.
- Petryk S, Bosmajin G. (1975), "Analysis of flow through vegetation", *J. Hydraulics Division, ASCE*, **V.101(7)**, pp.871-884.
- Righetti M, Armanini A. (2002), "Flow resistance in open channel flows with sparsely distributed bushes", *J. Hydrology*, **V.269**, pp.55-64.
- Sayah SM, Boillat JL, Schleiss A. (2004), "The use of soft shore protection measures in shallow lakes: Research methodology and case study", *Limnologica*, **V.34**, pp.65-74.
- Stokes KE. (2008), "Exotic invasive black willow (*Salix nigra*) in Australia: influence of hydrological regimes on population dynamics.", *Plant Ecol.*, **V.197**, pp.91-105.
- Technology Research Center for Riverfront Development (TRCRD). (1994), "Guideline for tree management in rivers (in Japanese)", Sankaidou, pp.154-160.
- Takemura T, Tanaka N. (2005), "Evaluation of expansion threshold for *Typha angustifolia* in river", *XXXI IAHR Congress*, pp.1884-1893.
- Takemura T, Tanaka N. (2007), "Flow structures and drag characteristics of a colony-type emergent roughness model mounted on a flat plate in uniform flow", *Fluid Dynamics Research*, **V. 39**, pp.694-710.
- Tanaka N, Sasaki Y, Mowjood MIM. (2006), "Effects of sand dune and vegetation in the coastal area of Sri Lanka at the Indian Ocean tsunami, In: Eds, Namsik Park et al., *Advances in Geosciences 6*", World Scientific Publishing, Co.
- Tanaka N, Ito S, Yagisawa J. (2008), "Flow structures and sedimentation characteristics around colony-type vegetation at flood events", *Proc. of 16th IAHR-APD & 3rd IAHR-ISHS*, pp.981-986.
- Tanaka N, Yagisawa J. (2008), "Differences of tree-breaking pattern and breaking moment by floods with different tree age and substrate condition under two flood disturbances", *8<sup>th</sup> International Conference on Hydro-Science and Engineering, Nagoya, Japan*, pp.473-474.
- Tanaka N, Yagisawa J. (2009), "Effects of tree characteristics and substrate condition on critical breaking moment of trees due to heavy flooding", *Landscape and Ecological Engineering*, **V.5(1)**, pp.59-70.
- Temple DM. (1980), "Tractive force design for vegetated channels", *Trans. ASAE*, **V.23(4)**, pp.884-890.
- Van de Wiel MJ, Darby SE. (2007), "A new model to analyse the impact of woody riparian vegetation on the geotechnical stability of

riverbanks”, *Earth Surf. Process. Landforms*, **V.32**, pp.2185-2198.

Vervuren PJA, Blom CWPM, Kroon HD. (2003), ”Extreme flooding events on the Rhine and the survival and distribution of riparian plant species”, *J. Ecology*, **V.91**, pp.135-146.

Wallerstein NP, Thorne CR. (2004), “Influence of large woody debris on morphological evolution of incised, sand-bed channels”, *Geomorphology*, **V.57**, pp.53-73.

Wyżga B. (2001), “Impact of the channelization-induced incision of the Skawa and Wisłoka Rivers, southern Poland, on the conditions of overbank deposition”, *Regulated Rivers: Research & Management*, **V.17**, pp.85-100.